JOURNAL OF GEOPHYSICAL RESEARCH, VOL. 102, NO. A9, PAGES 19,935–19,941, SEPTEMBER 1, 1997

An empirical model of the substorm current wedge

Nikolai A. Tsyganenko

Hughes STX Corporation, Laboratory for Extraterrestrial Physics, NASA Goddard Space Flight Center
Greenbelt, Maryland

Abstract.

A wedge-shaped current linking the nightside ionosphere and the plasma sheet is believed to be the principal cause of a major reconfiguration of the magnetospheric field on the nightside, observed at the onset of the substorm's explosive phase. No dynamical model of the magnetosphere is complete without this important component; however, no realistic representation for the field of the substorm current wedge has been available so far, in part due to the geometrical complexity of that current system and related computational problems. In this work, a simple and flexible analytical model is proposed for the magnetic field of substorm current wedge. The key element of the mathematical treatment is the vector potential of the field produced by a pair of current loops with a spread-out volume current density. Applying appropriate shift, rotation, and a minor stretching deformation makes it possible to reproduce the desired geometry of the entire system, including field-aligned currents. The current wedge has a variable longitudinal width, and the model is further generalized by including warping effects due to the tilt of Earth's dipole. This model is intended to be used in data-based representations of the magnetic field dynamics in the near magnetosphere and will make it possible to reproduce the fast restructuring of the near-Earth field during the explosive phase of a substorm.

1. Introduction

The concept of the substorm current wedge (SCW) was suggested in the early seventies, based on an extensive evidence from space- and ground-based magnetic field observations during the expansion phase of magnetospheric disturbances [e.g., *McPherron et al.*, 1973, *Clauer and McPherron*, 1974]. These observations suggested that an essential feature of a substorm was a sudden disruption of a part of the cross-tail current and its redirection along geomagnetic field lines, with downward and upward Birkeland currents concentrated on the dawn and dusk sides of the disturbance sector, respectively, [e.g., *Lui et al.*, 1992, *Lopez and Lui*, 1990]. The rapid disruption of the cross-tail current in a localized region on the nightside and its divertion via field-aligned currents to low altitudes is equivalent to a buildup of a three-dimensional wedge-shaped curcuit with a limited longitudinal extent, as schematically shown in Figure 1. The total current in the SCW can be quite large, resulting in a major reconfiguration of the magnetic field on the nightside, with a local collapse of previously stretched field lines to a quasi-dipolar configuration.

Quantitative studies of substorm effects often require a realistic model of the magnetic field, capable of replicating the main effects of the SCW. However, although the concept of the SCW has existed for many years, no consistent quantitative model of that current system has been developed so far, mainly for two reasons. First, the configuration, size, and the local time position of the SCW can vary widely from one event to another, and even during the same substorm [*Lopez and Lui*, 1990]. Hence it is difficult, if at all possible, to define the parameters of an "average" SCW, based on the combined data from many substorms. Second, due to the complex geometry of the SCW, it is not easy to devise a reasonably simple and flexible mathematical model of the SCW disturbance field. *Horning et al.* [1974] constructed a simple wire model, using Biot-Savart integration over line currents, and fitted it to the data from eight low-latitude ground stations and the ATS-1 satellite.

Vasilyev et al. [1986] were first to relate the magnetic effects of the SCW to the formation of the auroral bulge. They mapped equatorial cross sections of the near tail, running from dawn to dusk, by using a background model field with added disturbance field from a simple line-current wedge model, and found a bulge-like deformation of the ionospheric projection, caused by the twisting effect of the Birkeland currents upon the magnetic field line [see also *Kaufmann et al.*, 1990; *Lyons et al.*, 1990, 1991].

Hilmer and Voigt [1995] suggested modeling the magnetic effects of the SCW by adding to the background magnetic field model a disturbance field from an eastward current sheet with a limited extension in the dawn-dusk and tailward-sunward directions. Although they were able to reproduce the observed dipolarization of the nightside field, the equatorial current in their model extended out into the tail lobes, instead of closing in the ionosphere via localized Birkeland currents. That limitation did not allow a strong B_y disturbance to arise, as is typically observed on the nightside during the substorm expansion phase.

The purpose of the present work is to suggest a mathematically simple and flexible representation for the SCW,

Paper number 97JA01904.
0148-0227/97/97JA-01904$09.00

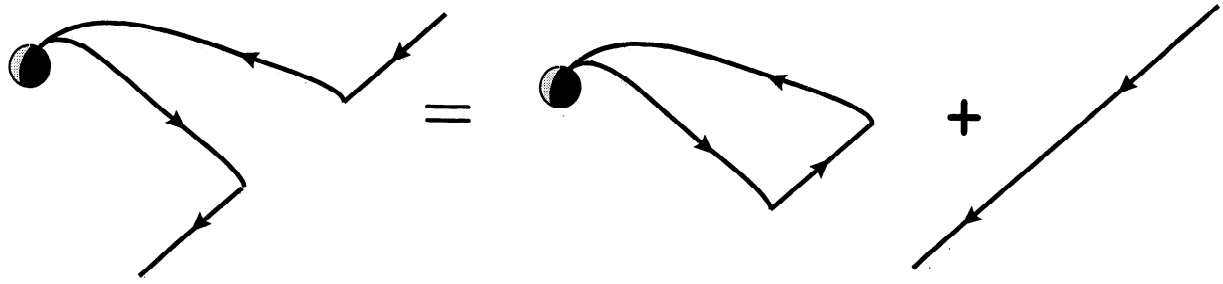

Figure 1. A sketch illustrating the concept of a substorm current wedge (SCW), confined within a limited interval of longitude.

which could be used in the development of a versatile dynamical data-based model of the disturbed magnetosphere during substorms.

2. Approach

The accuracy and realism of models of any complex physical object, based on large amounts of experimental data, depends crucially on two things. First, one needs a certain amount of a priori knowledge on the object's structure and its dependence on external conditions. At the very least, its qualitative structure must be guessed, in order to allow an appropriate choice of the mathematical frame for the model. Second, the model must include a sufficient amount of freedom, so that a good fit to observations could be obtained, with minimal and random residual differences between the model and data. The magnetospheric magnetic field depends not only on $\{x, y, z\}$ but also on additional varying parameters (the geodipole tilt angle, solar wind characteristics, and activity indices), and therefore the problem amounts to the multidimensional fitting of a vector function to large numbers of data points.

This imposes another requirement on the mathematical frame of a model: not only should it be realistic and flexible but also sufficiently simple. In this regard, the numerical computation of the field, based on the Biot-Savart law, is of little help, unless the integration can be carried out in quadratures, which is possible only for a few simple distributions of electric current.

With regard to modeling highly variable substorm current systems, an additional aspect becomes important: due to a very dynamical nature of the disturbances and a relatively small number of available simultaneous data, one can expect to fit meaningfully only a few parameters of the SCW, reflecting its most important characteristics. This also requires the model to be relatively simple.

In some cases it is possible to obtain simple analytical solutions for the magnetic field $\vec{\mathbf{B}}$ with a desired distribution of the electric current $\vec{\mathbf{j}} = \nabla \times \vec{\mathbf{B}}$ by modifying and superposing some simple "nucleus" solutions for the vector potential, having appropriate asymptotic properties. For example, the spread-out model of the ring current by *Tsyganenko and Usmanov* [1982] was derived by adding a constant term in the denominator of the vector potential of the dipolar magnetic field. The tail current sheet models, developed in our earlier works [*Tsyganenko,* 1989; *Tsyganenko and Peredo,* 1994; *Tsyganenko,* 1995], were based on simple analytical vector potentials for the field of infinitely thin current discs with different rates of outward decrease of the current strength. In that case, simple modifications of the original nucleus potentials made it possible to give the current sheet a controllable finite thickness and to warp it in response to the Earth's dipole tilt. Note that since $\vec{\mathbf{B}} = \nabla \times \vec{\mathbf{A}}$, any modification of vector potentials does not violate the condition $\nabla \cdot \vec{\mathbf{B}} = 0$.

To devise a model for the substorm current wedge, we use the vector potential of a circular current loop, shown in Figure 2a, as the initial "nucleus" solution. The basic idea is to combine two identical loops, symmetrically tilted with respect to the midnight meridian plane, shift them tailward, so that the currents flow nearly along the dipolar field lines at close geocentric distances (Figure 2b), and introduce a variable finite thickness of the current loops by a simple modification of the vector potential.

Expressed mathematically, the representation starts from the well-known relation in the cylindrical coordinates $\{\rho, \phi, z\}$ for the vector potential of a circular current loop of radius R_0 shown in Figure 2a [e.g., *Smythe,* 1950; *Jackson,* 1962]:

$$\vec{\mathbf{A}} = A_\phi \vec{\mathbf{e}}_\phi \qquad A_\phi = \frac{\left(1 - \frac{k^2}{2}\right)K(k) - E(k)}{k\sqrt{\rho}}, \quad (1)$$

where

$$k^2 = \frac{4R_0\rho}{(R_0 + \rho)^2 + z^2}, \qquad \rho = \sqrt{x^2 + y^2} \quad (2)$$

The argument k of the elliptical integrals $E(k)$ and $K(k)$ varies within the limits $0 \leq k \leq 1$, and the exact equality $k = 1$ is reached when the observation point lies on the loop, $\rho = R_0$, $z = 0$, at which point the function $K(k)$ becomes logarithmically singular. A simple and obvious way to spread out the infinitely thin current loop is to eliminate the singularity by adding a positive term D^2 to the denominator in the right-hand side of (2). At large distances from the loop, the modification does not significantly change the magnetic field, and it remains there virtually current-free. In the vicinity of the loop, however, the initially delta-like current becomes smoothly distributed in space around its original position.

The next step is to shift the loop along the x-axis, incline it by an angle γ to the equatorial plane, and combine it with another loop with the same radius and strength of the current, but rotated in the opposite direction around the x-axis, as shown in Figure 2b. The resultant current system is qualitatively similar to the SCW in its geometrical structure. In order to bring it closer to the expected one, several modifications are carried out.

First, the vector potential $\vec{\mathbf{A}}$ is stretched in the day-night direction in a way similar to that suggested by *Stern* [1987],

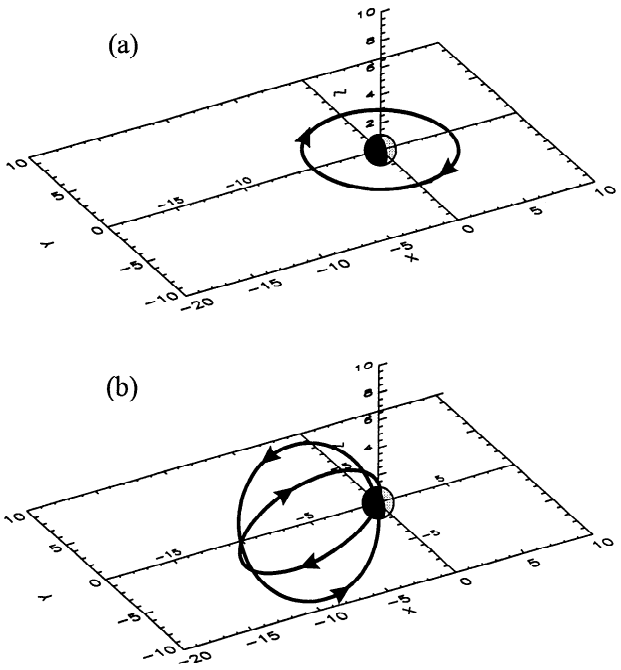

Figure 2. Three-dimensional views, illustrating the method of constructing the simple SCW model: (a) a single loop in the equatorial plane; (b) a combination of two circular current loops, providing the prototype magnetic field for the SCW model.

in order to deform the electric current flow lines and bring them closer to the shape of the quasi-dipolar magnetic field lines on the nightside. To do so, it suffices to replace x in the vector potential (1) by a stretched coordinate $f(x)$. We have chosen $f(x)$ in the form

$$f(x, y, z) = x\left(1 - \frac{\alpha}{1 + r^2/R_s^2}\right) \tag{3}$$

where $r^2 = x^2 + y^2 + z^2$. The parameters α and R_s control the degree of the stretch and its radial extent, respectively. The stretch is maximal near the origin and falls off to zero at large radial distances, as $r \gg R_s$. For the specific form (3) of the stretch function $f(x, y, z)$, the length of the major semiaxis of the stretched loop, x_d, can be found in a closed analytical form from the equation $f(x, 0, 0) = R_0$. Denoting $x/R_s \equiv t$ and $R_0/R_s \equiv \beta$, one can obtain x_d as a solution of a cubic equation $t^3 - \beta t^2 + (1 - \alpha)t - \beta = 0$, in the form

$$x_d = -R_s\left[\frac{\beta}{3} + \sqrt[3]{-\frac{q}{2} + \sqrt{Q}} + \sqrt[3]{-\frac{q}{2} - \sqrt{Q}}\right] \tag{4}$$

where

$$q = -\frac{\beta}{3}\left[2\frac{\beta}{3}^2 + \alpha + 2\right] \qquad Q = \left(\frac{p}{3}\right)^3 + \left(\frac{q}{2}\right)^2$$

$$p = 1 - \alpha - \frac{\beta^2}{3}$$

Thus defined x_d is the distance by which the loops must be shifted in the negative x-direction, in order to approximately align the currents with the dipolar field lines near Earth. Note that in this model we do not require the field-aligned currents to close within a thin ionospheric layer, but assume that the westward closure current at low altitudes is spread-out over a larger interval of geocentric distances; this question will be discussed in more detail in section 4.

Second, in order to match the geometry of the model SCW with the one expected from the general quasi-dipolar structure of the near-Earth magnetic field, the characteristic half-thickness of the currents, D, is made to depend on the position of the observation point along the x-axis. This results in a variable transverse dimension of the current flow, so that it is confined within a narrow flux tube at low altitudes, but spreads outward and reaches its widest, as the flow lines reach the equatorial plasma sheet and cross there the midnight meridian plane. More specifically, the function $D(x)$ entering in the modified argument

$$k^2 = \frac{4R_0\rho}{(R_0 + \rho)^2 + z^2 + D^2(x)} \tag{5}$$

is assumed to have the form

$$D(x) = -D_0 \tanh\frac{x}{\Delta x} + \delta \tag{6}$$

According to (6), the current flow line tubes widen with increasing tailward distance and narrow down to the ionosphere. It is important to note that the formulas (1)–(6) directly define the magnetic field produced by the spread-out currents, rather than the electric current density, and, therefore, the coordinates $\{x, y, z\}$ entering in the vector potential and in the magnetic field components refer to the observation point, which can be located anywhere in space. With increasing positive values of x on the dayside, the thickness D in (6) falls off to zero and then becomes negative; however, it does not cause a singularity or other problem, since the shifted current loops reside entirely on the nightside and hence the argument k^2 given by (5) never reaches unity.

Figure 3 shows a three-dimensional view of the electric current flow lines in the model SCW, with $\gamma = 55°$, $D_0 = 2R_E$, $\Delta x = 7R_E$, and $\delta = 0.2R_E$. The apparent sharp kinks in flow lines south of the equator are merely effects of the viewing angle: actually those lines are mirror images of the northern ones. Because the original thin loops were spread out, the current smoothly flows from one loop into the other across the midnight meridian plane and, thanks

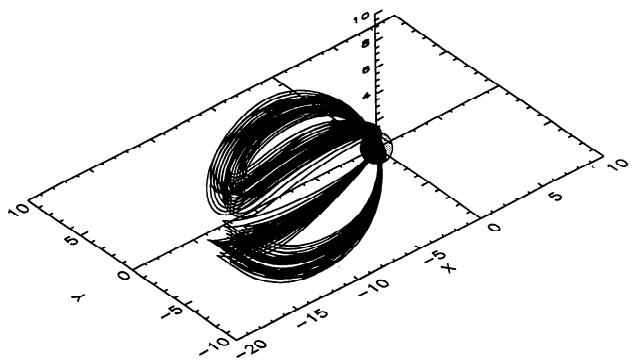

Figure 3. Electric current flow lines in the SCW model, obtained by spreading out the current and tailward stretching of the field from the prototype double-loop system shown in Figure 2b. The apparent kinks on the lines south of the equator are due to effects of the viewing angle.

to the symmetry, no current crosses the equator. Besides the total electric current in the wedge, the model has several variable geometrical parameters: the radius R_0, defining the overall size of the SCW, the stretch amplitude α, the angle γ controlling the width of the SCW in longitude, and the azimuthal position of the SCW.

If the current disruption on the nightside occurs relatively close to Earth, one can assume that the SCW tends to follow quasi-dipolar magnetic field and hence its position is best defined in the solar magnetic coordinates, whose z-axis is aligned with the axis of the geodipole magnetic moment. However, the radial extent of the SCW is highly variable (A. T. Y. Lui, private communication, 1997), so that in a general case one has to take into account the warping of the nightside magnetic configuration, due to diurnal and seasonal change of the inclination of the Earth's dipole axis to the terminator plane (or the tilt angle Ψ). These effects are addressed in section 3.

3. Warping Effects Related to the Geodipole Tilt

In the general case $\Psi \neq 0$, the limitation of the north-south symmetry should be removed, which can be done by introducing a radially dependent warping of the vector potential. We begin with replacing the unwarped Cartesian solar magnetospheric coordinates $\{x, y, z\}$ by the warped ones, $\{x^*, y^*, z^*\}$, which coincide with the solar-magnetic coordinates at the Earth's surface and asymptotically approach the solar magnetospheric coordinates with growing radial distance r. A convenient and simple specific form for the warped coordinates was suggested in an earlier work [*Tsyganenko and Stern*, 1996] as

$$\begin{aligned} x^* &= x\cos\Psi^*(r) - z\sin\Psi^*(r) \\ y^* &= y \\ z^* &= x\sin\Psi^*(r) + z\cos\Psi^*(r) \end{aligned} \tag{7}$$

where the radially varying warp angle Ψ^* is related to the geodipole tilt angle Ψ by

$$\sin\Psi^*(r) = \frac{C(r)}{C(1)}\sin\Psi \tag{8}$$

The function $C(r)$ in (8) was chosen in a simple form, providing a smooth transition from $\Psi^* = \Psi$ at $r = R_E$ to $\Psi^* = \sin^{-1}(R_H/r)$ for $r \to \infty$:

$$C(r) = \frac{\sqrt{(R_H + r)^2 + \Delta R^2} - \sqrt{(R_H - r)^2 + \Delta R^2}}{r} \tag{9}$$

with the "hinging distance" $R_H = 9R_E$ and the warp scale distance $\Delta R = 3R_E$. For zero dipole tilt, $\Psi = 0$, the warped coordinates (7) are reduced to the original solar magetospheric ones. The lines of warped coordinates $\{x^*, z^*\}$ were calculated elsewhere (see Figure 3 of *Tsyganenko and Stern* [1996]) and are not reproduced here.

In constructing the warped vector potential, $\vec{\mathbf{A}}^{(w)}$, it was assumed that its components retained the same functional dependence on the position $\{x^*, y^*, z^*\}$ in the space of warped coordinates, as in the unwarped case, and obeyed the same transformation relations (7), as the components of the position vector. From this, the following procedure was defined. First, we replace unwarped coordinates $\{x, y, z\}$ in the original vector potential $\vec{\mathbf{A}}$ by the warped ones from (7) and obtain the components of $\vec{\mathbf{A}}^{(w)}$ in the warped coordinate system as

$$\vec{\mathbf{A}}^*(x, y, z) = \vec{\mathbf{A}}(x^*, y^*, z^*) \tag{10}$$

After that, we apply the inverse transformation to the components of the potential $\vec{\mathbf{A}}^*$ and obtain the components of the warped vector potential in the original (GSM) coordinate system as

$$\begin{aligned} A_x^{(w)} &= A_x^*\cos\Psi^*(r) + A_z^*\sin\Psi^*(r) \\ A_y^{(w)} &= A_y^* \\ A_z^{(w)} &= -A_x^*\sin\Psi^*(r) + A_z^*\cos\Psi^*(r) \end{aligned} \tag{11}$$

In specifying the above procedure of the tilt-related space-warping, we did not use any physical assumptions, constraints, or other quantitative criteria (e.g., such as the stress balance). Rather, it was based merely on a conjecture that, for relatively small dipole tilt angles Ψ, the response of the electric current system and its magnetic field to changes in Ψ can be reduced to simple geometrical transformation of the vector potential. Therefore the above procedure needs an a posteriori justification by means of calculating the electric current $\vec{\mathbf{j}}$ for $\Psi \neq 0$ and comparing the resultant warped distribution of the current density with that for the case $\Psi = 0$. In doing so, two things should be checked. First, the warping of the vector potential inevitably gives rise to artificial distributed currents outside of the current wedge, which should be kept at a reasonably low level. Second, one can expect that the the total current in the wedge is relatively insensitive to the dipole tilt angle.

Testing of the warped SCW model gave satisfactory results. The electric current flow pattern was found to be close to the expected one, without major spurious currents, as illustrated by the contour maps of j_y and j_x distributions for the case of the dipole tilt of $\Psi = 20°$ in Figure 4. The left panel displays the contour maps of $-j_y$, i.e. of the current flowing across the noon-midnight meridian plane in the dusk-dawn direction. The dusk-dawn current is confined within a localized region in the near-tail plasma sheet and, for the given set of model parameters, the current density peaks at $X_{GSM} \approx -11R_E$. The low-altitude closure currents flow in the opposite direction (from dawn to dusk) and are concentrated within a much narrower region in the vicinity of Earth. Because of the conservation of the total current, they have much larger amplitude and are not shown in the plot because of their much smaller spatial scale. The right panel shows the contour plots of j_x in the plane $X_{GSM} = -5R_E$, parallel to the dawn-dusk meridian plane. Two pairs of Birkeland currents are clearly visible; the ones in the southern hemisphere have larger volume current density, because they are closer to Earth due to the positive dipole tilt.

4. Discussion

In this section we discuss in more detail the effects of the disturbance magnetic field as reproduced by the present model and point out its limitations. Figure 5 (left) shows the plots of the equatorial B_z from the model SCW for different

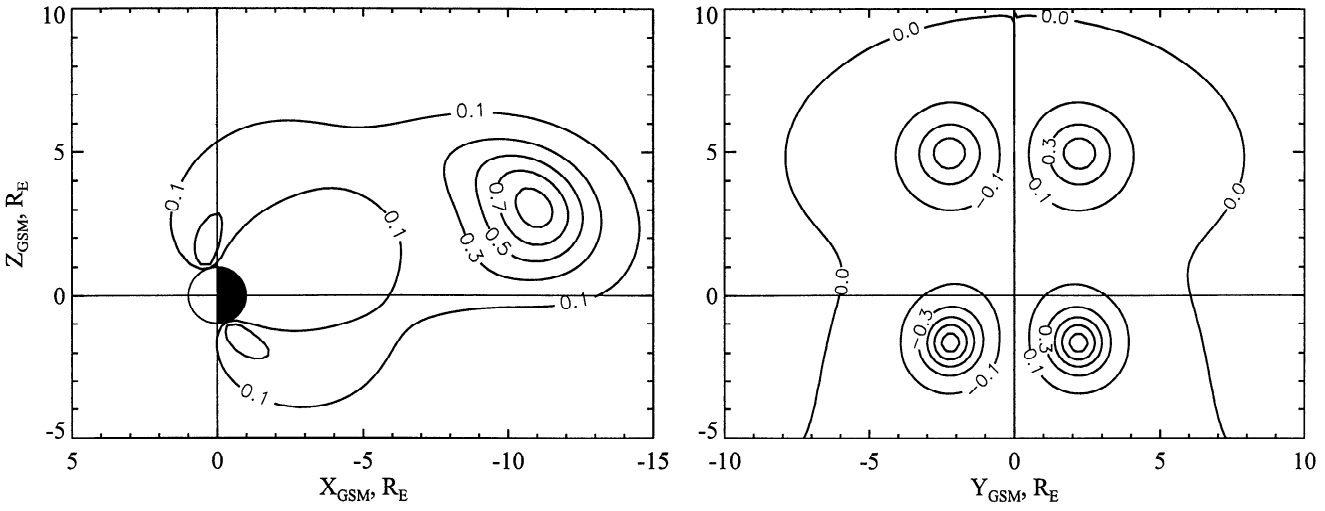

Figure 4. Contour maps of the electric current density distribution in the SCW model. (left) The distribution of j_y in the noon-midnight meridian plane; strong westward closure current near Earth is not shown, because of its much smaller spatial scale. (right) The distribution of j_x in the cross section of the tail at $X_{GSM} = -5R_E$. Two pairs of spread-out field-aligned currents are clearly seen as concentric circular contours.

values of the inclination angle γ, defining the longitudinal extent of the wedge. The total current in the double loop system is the same in all the cases and equals $\approx$ 550 kA, which provides a disturbance of $B_z \approx 10$ nT inside of the SCW with $\gamma = 55°$. As expected, smaller inclination angles γ (i.e., larger longitudinal extent of the wedge) correspond to larger disturbance field inside the current system. The disturbance is nearly constant inside the distant part of the wedge, but rapidly increases earthward at distances $r < 5R_E$. This is a consequence of our tacit assumption that the most part of the disrupted current is redirected along the field lines and extends all the way down to ionospheric altitudes. However, we still have no data that could either support or refute the assumption of fully ionospheric closure of the equatorial current. As noted by *Vasilyev et al.* [1986], the rapid buildup of the SCW is actually a complex dynamical process, which probably involves the formation of a steep Alfven wave with associated strong polarization currents across the magnetic field, propagating from the disruption region toward Earth. Therefore one should be aware that the electric current geometry like that in Figure 1 is a theoretical conjecture, reflecting only gross features of the real phenomenon. In that regard, empirical SCW models should have sufficient flexibility, in order to be able to replicate temporal evolution of the SCW structure. The present model allows to control the amount of electric current that reaches low altitudes, by varying the parameters of the function $D(x)$ in (6). In the right panel of Figure 5, the plots of $B_z(x)$ are shown, similar to those in the left panel, but with $D_0 = 0.8$ and $\delta = 1.2$. Because of the larger value of $D(x)$ near Earth, the field-aligned currents close at higher altitudes, which results in a more uniform radial distribution of the disturbance field. Note that, according

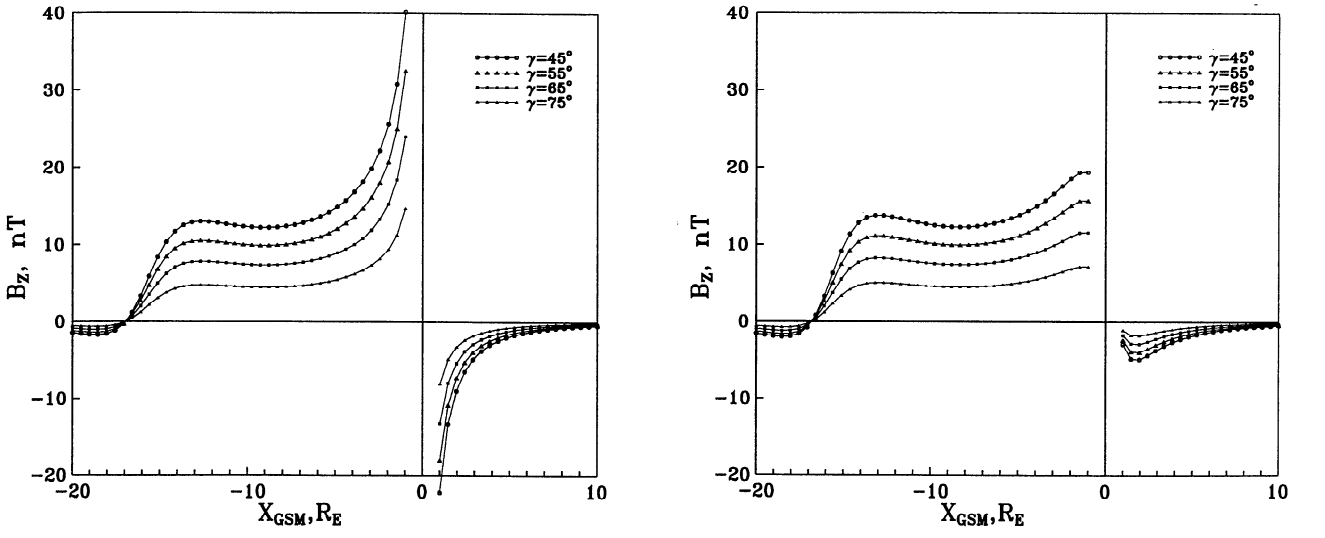

Figure 5. Plots of the SCW disturbance field (B_z) along the X_{GSM} axis, for four different values of the loop inclination angle. (left) Corresponds to $D_0 = 2$ and $\delta = 0.2$ (near-Earth closure of the SCW via field-aligned currents). (right) Corresponds to $D_0 = 0.8$ and $\delta = 1.2$, providing a more distributed westward closure current at low altitudes.

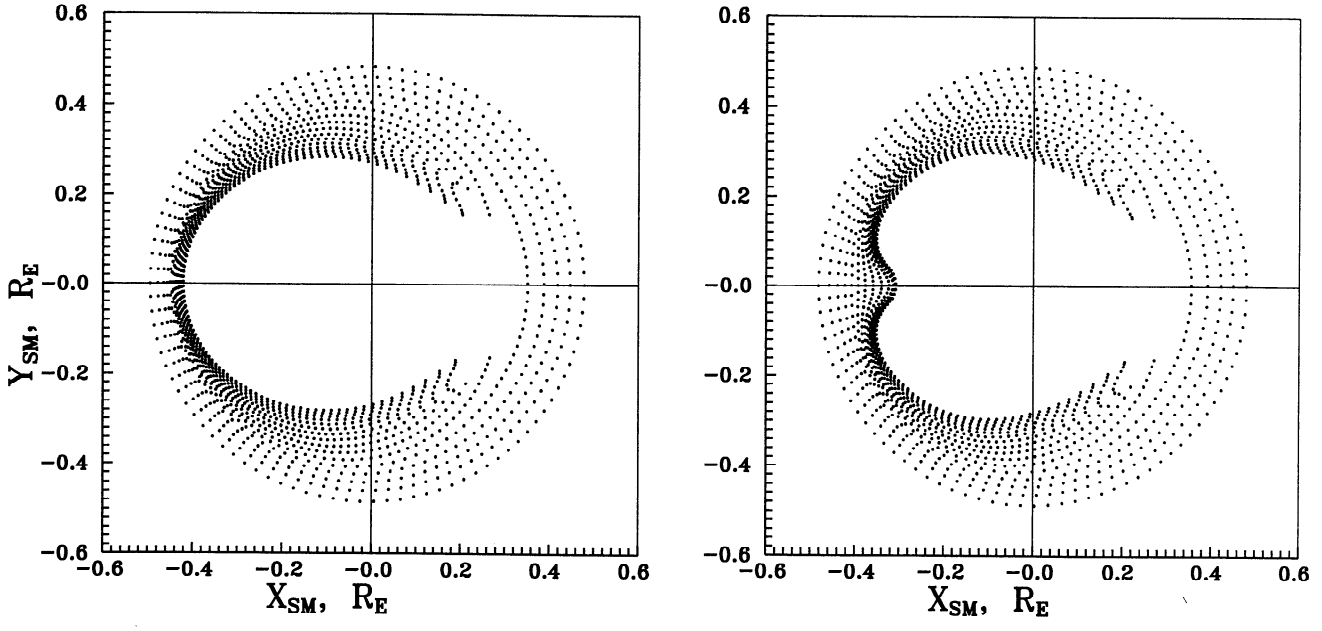

Figure 6. Ionospheric footpoints of model magnetic field lines, mapped from a family of 16 equidistant circles lying in the equatorial plane between $R = 5R_E$ and $R = 20R_E$. (left) No SCW. (right) A SCW with I_{tot} =1080 kA is turned on; due to tranverse field perturbation by field-aligned currents, a bulge is formed near midnight.

to observations of the substorm onset, the positive excursions of the H component at low-latitude ground stations have approximately the same amplitude as those at the geostationary orbit [e.g., *Nagai,* 1982]. This disagrees with the strong earthward increase of B_z in the left panel of Figure 5, found under assumption of the near-Earth closure of the disrupted tail current and supports the assumption of a more spread-out closure current, distributed over a larger range of altitudes.

By superposing several SCW models, shifted in longitude and having different parameters, it is in principle possible to obtain a wide variety of model substorm current systems, which can be fitted to simultaneous data of several spacecraft, spanning the nightside magnetosphere.

As was pointed out by *Vasilyev et al.* [1986] and *Lyons et al.* [1990, 1991], assuming the SCW model in the form of the "Birkeland current loop" allows to explain in terms of magnetic mapping the formation of the auroral bulge during substorms. To study that effect in more detail, the present SCW model was combined with the last version of the global field model [*Tsyganenko,* 1996] and the resultant field was used for mapping of a set of concentric circles in the equatorial plane along magnetic field lines to the ionosphere. Figure 6 shows the result of that calculation for $\gamma = 55°$ and two values of the total current in the SCW, I_{tot} =0, and I_{tot} =1080 kA, corresponding to the disturbance in the B_z component inside the SCW equal to 0 nT and 20 nT, respectively. In both cases, the field of the SCW was added to the background field given by T96_01 model with the following values of input parameters: solar wind pressure P=4 nPa, Dst=-40 nT, IMF B_y = 2 nT, and B_z = −5 nT, simulating conditions during the growth phase of a substorm. As can be seen in the right panel, a conspicuous bulge is formed on the nightside,

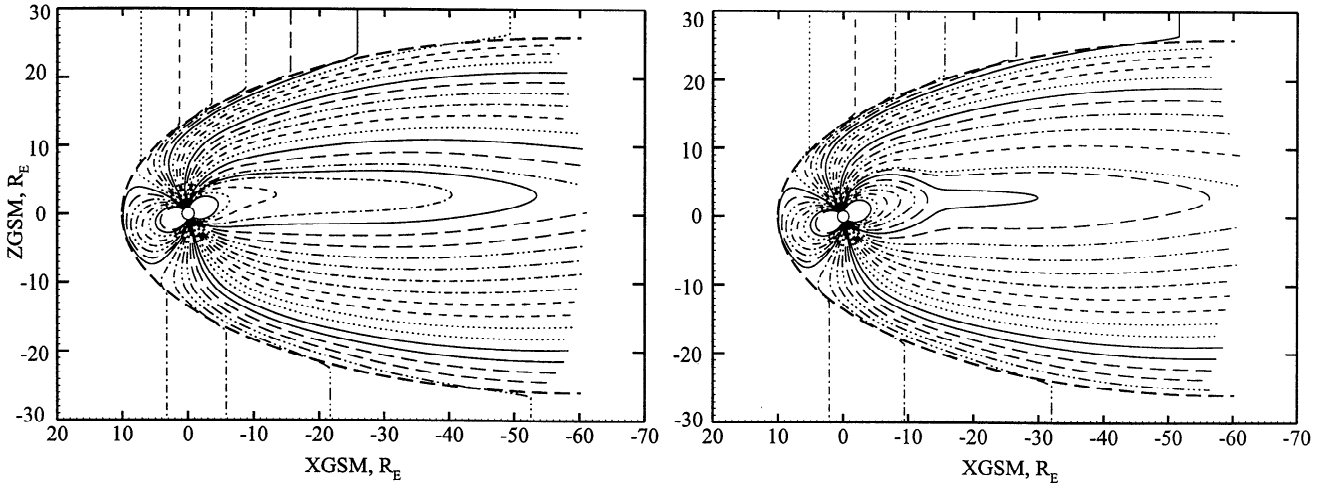

Figure 7. Mapping of model field lines in the noon-midnight meridian plane, illustrating the effect of the SCW-related dipolarization of the nightside magnetic field. (a) No SCW field (a prebreak-up configuration); (b) A SCW with I_{tot}=1080 kA is turned on. Field lines having the same values of the footpoint latitude are displayed by using the same linestyle.

resembling the well-known characteristic feature of auroral activity during the expansion phase of a substorm.

Figure 7 shows two noon-midnight plots of field line configurations, corresponding to the cases of (1) $I_{tot} = 0$ in the SCW (left plot in Figure 6, end of the growth phase), and (2) $I_{tot} = 1080$ kA (right plot in Figure 6, onset of an expansion phase). The configurations do not represent any specific event and are given just for illustrating the effect of the SCW on the global field geometry. Field lines with different footpoint latitudes were plotted using different line styles, in order to better demonstrate the effect of a dramatic collapse of the field lines towards a more dipolar configuration.

The representation of the SCW magnetic field, described above, is intended to be used with the model of the average global field, in order to simulate transient reconfigurations of the nightside field during the substorm expansion phase. The model is analytically simple and contains a few parameters, which can be fitted to spacecraft data. However, as already noted above, the statistical approach, used for constructing the global field models, may be not feasible for the derivation of the SCW parameters, due to a large variability of the disturbed field from one substorm to another. The most effective way of implementing the SCW model would be the "event-oriented" modeling, based on fitting to data, taken simultaneously at several different locations by a constellation of spacecraft. First attempts have already been made to apply that method for studying the magnetic configurations during the growth and recovery phases of a substorm [*Pulkkinen et al.*, 1992, 1994].

With the advent of the era of multispacecraft missions, one can expect a substantial progress in the studies of the dynamical evolution of the global disturbed magnetosphere. Using simultaneous data from many spacecraft, covering the near tail region, it will be possible to determine the parameters of the tail and SCW in real time and use them for constructing consecutive snapshots of the evolution of the global magnetic field.

Acknowledgments. The author thanks Victor Sergeev for pointing out important previous works on the SCW and David Stern for his careful reading of the preliminary version of this paper and many helpful comments. This work is supported by NASA grant NAS5-32350 and NSF Magnetospheric Physics Program grant ATM-9501463.

The Editor thanks L.R. Lyons and M.A. Heinemann for their assistance in evaluating this paper.

References

Clauer, C.R., and R.L. McPherron, Mapping the local time-universal time development of magnetospheric substorms using midlatitude magnetic observations, *J. Geophys. Res., 79*, 2811–2820, 1974.

Hilmer, R.V., and G.-H. Voigt, A magnetospheric magnetic field model with flexible current systems driven by independent physical parameters, *J. Geophys. Res., 100*, 5613–5626, 1995.

Horning, B.L., R.L. McPherron, and D.D. Jackson, Application of linear inverse theory to a line current model of substorm current systems, *J. Geophys. Res., 79*, 5202–5210, 1974.

Jackson, *Classical Electrodynamics*, 641 pp., John Wiley, New York, 1962.

Kaufmann, R.L., D.J. Larson, and C. Lu, Mapping and distortions of auroral structures in the quiet magnetosphere, *J. Geophys. Res., 95*, 7973–7994, 1990.

Lopez, R.E., and A.T.Y. Lui, A multisatellite case study of the expansion of a substorm current wedge in the near-tail magnetotail, *J. Geophys. Res., 95*, 8009–8017, 1990.

Lui, A.T.Y., R.E. Lopez, B.J. Anderson, K. Takahashi, L.J. Zanetti, R.W. McEntire, T.A. Potemra, D.M. Klumpar, E.M. Greene, and R. Strangeway, *J. Geophys. Res., 97*, 1461–1480, 1992.

Lyons, L.R., O. De La Beaujardiere, G. Rostoker, J.S. Murphree, and E. Friis-Christensen, Analysis of substorm expansion and surge development, *J. Geophys. Res., 95*, 10,575–10,589, 1990.

Lyons, L.R., Association between tail substorm phenomena and magnetic separatrix distortion, in *Magnetospheric Substorms, Geophys. Monogr. Ser.*, vol. 64, edited by J.R. Kan, T.A. Potemra, S. Kokubun, T. Iijima, pp. 161-170, AGU, Washington, D.C., 1991.

McPherron, R.L., C.T. Russell, and M.P. Aubry, Satellite studies of magnetospheric substorms on August 15, 1968, 9, Phenomenological model for substorms, *J. Geophys. Res., 78*, 3131–3149, 1973.

Nagai, T., Observed magnetic field signatures at synchronous altitude, *J. Geophys. Res., 87*, 4405–4417, 1982.

Pulkkinen, T.I., D.N. Baker, R.J. Pellinen, J. Buchner, H.E.J. Koskinen, R.E. Lopez, R.L. Dyson, and L.A. Frank, Particle scattering and current sheet stability in the geomagnetic tail during the substorm growth phase, *J. Geophys. Res., 97*, 19283–19297, 1992.

Pulkkinen, T.I., D.N. Baker, P.K. Toivanen, R.J. Pellinen, R.H.W. Friedel, and A. Korth, Magnetic field and current distribution during the substorm recovery phase, *J. Geophys. Res., 99*, 10955–10966, 1994.

Smythe, W.R., *Static and Dynamic Electricity*, McGraw-Hill, New York, 1950.

Stern, D.P., Tail modeling in a stretched magnetosphere, 1, Methods and transformations, *J. Geophys. Res., 92*, 4437–4448, 1987.

Tsyganenko, N.A., A magnetospheric magnetic field model with a warped tail current sheet, *Planet. Space Sci., 37*, 5–20, 1989.

Tsyganenko, N.A., Modeling the Earth's magnetospheric magnetic field confined within a realistic magnetopause, *J. Geophys. Res., 100*, 5599–5612, 1995.

Tsyganenko, N.A., Effects of the solar wind conditions on the global magnetospheric configuration as deduced from data-based field models, in *Proceedings of Third International Conference on Substorms (ICS-3), Eur. Space Agency Spec. Publ., ESA SP-389*, 181–185, 1996.

Tsyganenko, N.A., and M. Peredo, Analytical models of the magnetic field of disk-shaped current sheets, *J. Geophys. Res., 99*, 199–206, 1994.

Tsyganenko, N.A., and D.P. Stern, Modeling the global magnetic field of the large-scale Birkeland current systems, *J. Geophys. Res., 101*, 27,187–27,198, 1996.

Tsyganenko, N.A., and A.V. Usmanov, Determination of the magnetospheric current system parameters and development of experimental geomagnetic field models based on data from IMP and HEOS satellites, *Planet. Space Sci., 30*, 985–998, 1982.

Vasilyev, E.P., M.V. Malkov, and V.A. Sergeev, Three-dimensional effects of a Birkeland current loop, *Geomagn. Aeron. Engl. Transl., 26*, 88–91, 1986.

N. A. Tsyganenko, Hughes STX Corporation, Laboratory for Extraterrestrial Physics, Code 695, NASA Goddard Space Flight Center, Greenbelt, MD 20771. (e-mail: kolya@nssdca.gsfc.nasa.gov)

(Received May 19, 1997; revised June 30, 1997; accepted July 1, 1997.)